

# Simultaneous multiple enantioseparation with a one-pot imprinted microfluidic channel by microchip capillary electrochromatography

Ping Qu, Jianping Lei, Jin Sheng, Lei Zhang and Huangxian Ju\*

Received 22nd July 2010, Accepted 10th November 2010

DOI: 10.1039/c0an00559b

A multi-template imprinted microchannel was prepared by a one-pot *in situ* imprinting process. The imprinted microchannel led to a novel chip-based strategy for simultaneous multiple enantioseparation. The one-pot imprinting process formed a multi-template imprinted porous thin layer (about 2  $\mu\text{m}$ ) on the inner wall of the capillary, which was characterized by scanning electron microscopy, infrared spectroscopy, and solid-state UV-vis spectroscopy. By fixing the imprinted capillary to a support substrate composed of poly(dimethylsiloxane) on a glass slide, a multi-analyte microchip was thus conveniently constructed. Using L-tyrosine (L-Tyr) and L-tryptophan (L-Trp) as the template molecules, two pairs of enantiomers were simultaneously baseline separated in a 6 cm separation channel within 120 s under the optimized preparation and electrochromatographic conditions. The separation showed excellent efficiency. The linear ranges for amperometric detection of four analytes using a carbon fiber microdisk electrode at +1.2 V (vs. Ag/AgCl) were from 20 to 500  $\mu\text{M}$  for racemic Tyr and Trp. This multi-template imprinting strategy could be expanded for simultaneous separation and detection of additional pairs of enantiomers within a short analytical time. It could open up a promising avenue for high-throughput screening of chiral compounds.

## Introduction

Amino acids are one of the most important types of molecules for living beings, and most of the amino acids exist as stereoisomers (D-form and L-form) arising from the chiral centre on their  $\alpha$  carbon.<sup>1</sup> The ratio of D/L-amino acids in foodstuffs is an indicator of the quality and nutritional value, for example, an increase in their levels means a decrease in the food quality.<sup>2</sup> Furthermore, D-amino acids are also physiologically active substances that often act as disease biomarkers in mammals.<sup>3,4</sup> For instance, D-aspartic acid is observed in various endocrine and neuroendocrine tissues and it regulates the hormonal synthesis and secretion in tissues.<sup>5,6</sup> However, the amounts of D-amino acids in mammalian tissues are extremely small in most cases, and its determination is usually interfered by large amounts of its L-enantiomers.<sup>7</sup> Thus, although the quantitation of amino acid enantiomers has attracted considerable attention in evaluating human health and production quality, the simultaneous analysis of multiple amino acid enantiomers is still one challenge in analytical methodologies.

Various analytical methods involving gas chromatography,<sup>8</sup> high-performance liquid chromatography (HPLC),<sup>9</sup> and capillary electrophoresis (CE)<sup>10,11</sup> have been reported for the detection of amino acid enantiomers. Although these methods show good performance, most of them are time-consuming (from 20 to 50 min),<sup>8-12</sup> and can detect only a few amino acid enantiomers. To decrease the reagent and sample consumption, chiral separation of amino acids has been performed using ligand exchange CE<sup>13</sup> and heart-cutting 2-dimension CE.<sup>14</sup> However, they could

not provide the sufficient resolution for desired separation, especially for structurally related amino acid enantiomers. Recently, microchip electrophoresis (MCE)<sup>15-18</sup> and microchip electrochromatography (MCEC)<sup>19,20</sup> have become the most promising technique for miniaturized enantioseparation.<sup>21-25</sup> For example, fast chiral separation of 1-(dimethylamino)-5-naphthalenesulfonyl (DNS) labeled amino acids has been realized using MCE with fluorescence detection by using highly sulfated cyclodextrins as chiral selectors,<sup>24</sup> and enantioseparation of *tert*-butoxycarbonyl-tryptophan (Boc-Trp) enantiomers has been performed using MCEC by imprinting Boc-L-Trp on the inner wall of microfluidic channel.<sup>25</sup> Here, using the *in situ* molecular imprinting technique, a multi-template imprinted microchannel was prepared, and a novel chip-based strategy was designed for simultaneous enantioseparation of multiple enantiomers using a disposable microchip.

With high selectivity and good binding affinity toward the target molecules, molecularly imprinted polymers (MIPs) have demonstrated the ability to separate chiral compounds.<sup>26,27</sup> The MIPs have been used for capillary electrochromatographic (CEC) separation of racemic naproxen,<sup>28</sup> ketoprofen,<sup>29,30</sup> ropivacaine,<sup>31</sup> and propranolol,<sup>32</sup> *etc.* Multi-template imprinted MIP nanoparticles have also been used for HPLC or CEC enantioseparation of two couples of chiral drugs.<sup>33-35</sup> However, these methods need an analysis time of about 20 min and do not achieve the simultaneous baseline separation. Although the simultaneous multiple enantioseparation has been achieved using MCE,<sup>24</sup> no quantitative result was reported, and the analytes had to firstly be derivatised with DNS, which led to inconvenience and sometimes the formation of interfering by-products and introduction of bulky labelling moiety,<sup>36</sup> and thus greatly limited the application of the reported method. In this work, the amperometric detection technique was combined with

Key Laboratory of Analytical Chemistry for Life Science (Ministry of Education of China), Department of Chemistry, Nanjing University, Nanjing, 210093, China. E-mail: hxju@nju.edu.cn; Fax: +86-25-83593593; Tel: +86-25-83593593

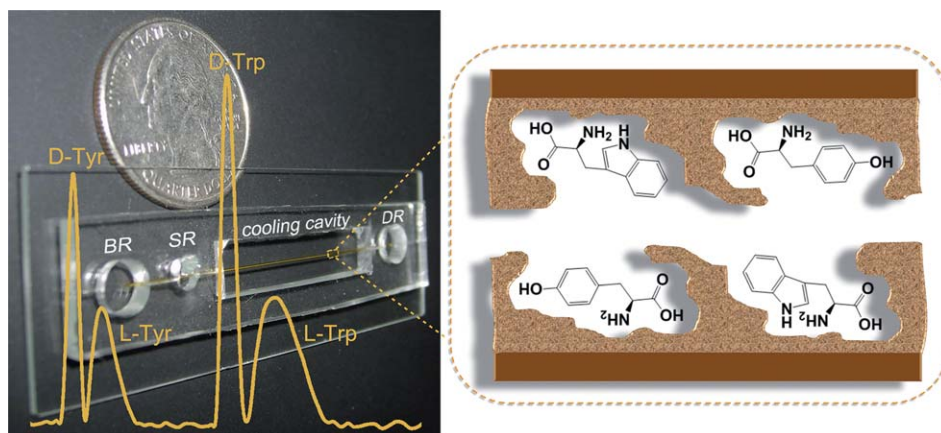


**Fig. 1** Photo of the imprinted microchip in comparison with one U.S. quarter together with the electropherogram for enantioseparation of two couples of enantiomers, and schematic representation of multi-template imprinted microchannel.

the multiple enantioseparation. The label-free method achieved the direct simultaneous detection of multiple enantiomers.

In view of the importance of trace D-tyrosine (D-Tyr) and D-tryptophan (D-Trp) in evaluating human health, they were selected in this work as the model enantiomers to prepare a multi-template imprinted microchannel with L-Tyr and L-Trp as templates by a one-pot imprinting technique. By fixing the imprinted capillary to a support substrate composed of poly-(dimethylsiloxane) (PDMS) on a glass slide, a multi-analyte microchip was conveniently constructed (Fig. 1). With this microchannel and a home-made carbon fiber microdisk electrode, the resulting microchip achieved simultaneous baseline enantioseparation and detection of racemic Tyr and Trp within 120 s. The D-Tyr and D-Trp showed better chromatographic performance and shorter analysis time than L-form. Considering a less than 0.39 nL sampling volume,<sup>37</sup> the designed method could detect the enantiomers down to 0.58 fmol, and be extended for simultaneous separation of more pairs of the structurally related amino acid enantiomers.

## Experimental

### Chemicals

L-Trp, D-Trp, L-Tyr, racemic Tyr, 3-(methacryloyloxy)propyl-trimethoxysilane ( $\gamma$ -MPS), acrylamide (AM) and ethylene glycol dimethacrylate (EDMA) were all purchased from Alfa Aesar (Ward Hill, MA). 2,2'-Azobisisobutyronitrile (AIBN) was obtained from Acros (Geel, Belgium). HPLC-grade acetonitrile (ACN) was supplied by Sigma-Aldrich (St. Louis, MO). Isooctane was supplied by Shanghai Chemical Reagent Co. (Shanghai, China). Quartz capillary with an inner diameter (i.d.) of 25  $\mu$ m and outer diameter (o.d.) of 365  $\mu$ m was purchased from Yongnian Optic Fiber Plant (Hebei, China). Sylgard 184 silicone elastomer and curing agent were purchased from Dow Corning (Midland, MI). Both the mobile phase and supporting electrolyte for MCE separation and amperometric detection were a mixture of ACN and acetate buffer filtered with 0.2  $\mu$ m membrane. All aqueous solutions were prepared using  $\geq 18$  M $\Omega$  ultrapure water (Milli-Q, Millipore).

### Equipment

Scanning electron micrographs (SEM) were obtained with a Hitachi S-4800 scanning electron microscope (Japan) at an acceleration voltage of 10 kV. Fourier transform infrared (FT-IR) spectra were recorded on a Nicolet 400 FT-IR spectrometer (Madison, WI). Solid-state UV-vis spectra were characterized with UV-3600 UV-vis-NIR spectrophotometer (Shimadzu, Kyoto). Ultrasonic disintegrator with a 2 mm o.d. probe from Ningbo Scientz Biotechnology (Ningbo, China) was used to prepare the sampling fracture on the separation capillary. Microinjection pump (Baoding Longer Precision Pump Co., Ltd., Shanghai, China) was used to operate the syringe. A laboratory-built high-voltage power supply controlled automatically by computer during experiments was used to supply separation voltage between 0 and +5000 V and sampling voltage between 0 and +1000 V, respectively. Electrochemical measurements were performed on a CHI 812 electrochemical station (CH Instruments Co.). For amperometric detection, a home-made carbon fiber microdisk electrode was prepared as working electrode (WE) and the detailed description of the electrode preparation was reported elsewhere.<sup>25</sup> A 40 multiple microscope (Nanjing Optics Instruments Factory, Nanjing, China) was employed to monitor the position of the WE.

### Preparation of multi-template imprinted microchannel

Prior to preparation, a quartz capillary (30 cm length) was flushed with 1 M NaOH followed by water for at least 30 min of  $\gamma$ -MPS and 1 mL 0.06 M acetic acid, and keeping the mixture in the capillary for 1.5 h. The silanized capillary was then flushed with water and dried with a flow of nitrogen. To avoid the formation of template-template complex,<sup>38</sup> the L-Tyr and L-Trp templates were firstly mixed with function monomer (AM) in porogenic mixture solvent (ACN and isooctane) for 10 h to form two template-monomer complex solutions, respectively, which were then mixed to form pre-polymerization solution by adding the cross-linker (EDMA) and initiator (AIBN) in the mixture. The composition of the pre-polymerization solution is shown in Table 1. The solution was pre-polymerized by sonication for 10 min, purged with nitrogen for 15 min to remove oxygen, and

**Table 1** Conditions for preparation of multi-imprinted microchannel<sup>a</sup>

No.	Amount of template/mmol		$I_s$		$\Delta t_R/s$
	L-Tyr	L-Trp	Tyr	Trp	
1	0.075	0.025	0.181	0.127	26.4
2	0.05	0.05	0.178	0.133	29.8
3	0.025	0.075	0.176	0.140	33.4

<sup>a</sup> All MIPs were prepared with 0.4 mmol AM, 2 mmol EDMA, and 24  $\mu$ mol AIBN in the mixture of 6 mL ACN and 280  $\mu$ L isooctane.

finally introduced to the capillary using a syringe for polymerization initiated thermally at 60 °C for 3 h. After polymerization, the capillary was flushed with ACN and methanol/acetic acid (9 : 1, v/v) using a syringe, respectively, to remove any unreacted reagent, and then cut into 6 segments for obtaining 4 separation microchannels with 6 cm length by abandoning two ends (3 cm length each). A non-imprinted polymer (NIP) modified capillary without template molecule was prepared using a similar process.

### Fabrication of microchip

The microchip was prepared by integrating the multi-template imprinted microchannel in a PDMS matrix (16 mm width and 67 mm length) as the support on a glass slide, which was prepared according to our previous work.<sup>39</sup> Before integration, one small scratch was made at the position of 0.5 cm from one end of the as-prepared capillary (6.0 cm length), at which the sampling fracture was formed by an ultrasonic probe after integration. The optimal ultrasonic conditions were 150 W with an action frequency of 12 times  $\text{min}^{-1}$  and a distance of 2 mm for 1 min.<sup>39</sup> The WE was mounted in a guide channel of the PDMS matrix, exactly opposite to the end of the separation channel. The Ag/AgCl reference electrode and Pt wire as auxiliary electrode were inserted to the detection reservoir (DR) to obtain an integrated three-electrode system for amperometric detection. The electrodes for performing the sampling were inserted into sample reservoir (SR) and buffer reservoir (BR), while the electrodes for separation were inserted into BR and DR.

### Enantioseparation of chiral compounds

The multi-template imprinted microchannel was firstly washed with the mobile phase. The fracture sampling was performed by applying an optimum injection voltage of 200 V between the SR and BR, and the separation voltage of 1200 V was applied to the BR with the DR grounded and the SR floating by automatically switching the high-voltage contacts. The electrochromatogram was recorded on a CHI 812 using the “amperometric  $i-t$  curve” mode at an applied potential of +1.2 V. The degree of enantiomer separation was represented by a normalized separation index ( $I_s$ ) with an equation:  $I_s = (t_{R2} - t_{R1})/t_{R1}$ , where  $t_{R1}$  and  $t_{R2}$  are the retention times ( $t_R$ ) of the first-eluting and the second-eluting enantiomers.<sup>33</sup> Resolution ( $R_s$ ) was calculated with  $R_s = 1.18(t_{R2} - t_{R1})/(W_{1/2(1)} + W_{1/2(2)})$ , where  $W_{1/2(1)}$  and  $W_{1/2(2)}$  are the peak width of the first-eluting and the second-eluting enantiomers at the half peak height, respectively.

## Results and discussion

### Imprinting conditions of microchannel

MIPs were prepared using an amide hydrogen-bonding functional monomer (AM) to form strong hydrogen-bonding interactions with the template molecules and create the specific recognition sites within the polymer matrix.<sup>40</sup> According to previous work,<sup>25</sup> the appropriate mole ratio between AM to template was 4 : 1, at which the resulting MIP showed the highest resolution of enantioseparation. At the AM amount of 0.4 mmol, the amounts of templates with a total amount of 0.1 mmol were firstly optimized in the presence of 2 mmol EDMA and 24  $\mu$ mol AIBN in 6 mL ACN and 280  $\mu$ L isooctane. The recognition properties of microchannels were characterized by the enantiomer separation degree, which was represented by  $I_s$ . As shown in Table 1, in the presence of two templates of Tyr and Trp, the  $I_s$  for Trp increased with the increasing ratio of L-Trp to L-Tyr. Similarly, the  $I_s$  for Tyr decreased with the increasing ratio of L-Tyr to L-Trp. More specific recognition sites formed in the MIP due to the more template<sup>33</sup> were in favor of the separation of the given enantiomers. However, compared with the change of  $\Delta t_R$ , the difference of retention times  $t_{R(D-Trp)}$  and  $t_{R(L-Tyr)}$ , which increased with the decreasing ratio of L-Tyr to L-Trp amounts and showed the maximum value at the ratio of 1 : 3, the change of  $I_s$  was relatively small. To achieve the simultaneous multiple enantioseparation, the amounts of 0.025 and 0.075 mmol for L-Tyr and L-Trp respectively were selected in the preparation of multi-template imprinted microchannel.

### Characterization of multi-template imprinted microchannel

The MIP could chemically attach on the silanol-rich inner surface of the silanized capillary. The SEMs of the MIP attached on the inner wall of the capillary are shown in Fig. 2. The bare capillary displayed a typical pillar structure with an inner diameter of 25  $\mu$ m (Fig. 2A and 2C), while the imprinted capillary showed a uniform layer of the MIP (Fig. 2B and 2D). The thickness of the MIP coating was about 2  $\mu$ m. A continuous skeleton morphology with relatively small rough pores could be

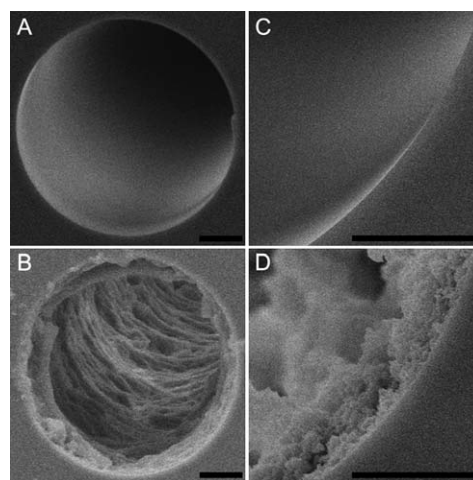


**Fig. 2** SEM images of (A, C) bare and (B, D) MIP-coated capillaries with two amplifications. The scale bars indicate 5  $\mu$ m.

observed (Fig. 2D). In addition, when the MIP-coated capillary was cut into many short pieces, the coating did not show any discontinuity at the cross-sections of the pieces. Thus, a three-dimensional imprinted porous polymer could be coated on the inner wall of the capillary to form an open-tubular capillary for selective recognition of enantiomers.<sup>29,30,41</sup> The resultant open-tubular capillary was easily flushed by a low voltage of 200 V to wash and to regenerate the surface.

To further characterize the Tyr/Trp-imprinted MIP (Tyr/Trp-MIP), FT-IR spectra of the functional monomer AM, the cross-linker EDMA, Tyr/Trp-MIPs before and after extraction, and NIP are compared in Fig. 3A. The spectrum of AM showed two absorption peaks at 3356 and 3184  $\text{cm}^{-1}$ , which were assigned to the N–H stretching vibration of the primary amide, while the C=C stretching vibration occurred at 1641  $\text{cm}^{-1}$ . The spectrum of EDMA showed a peak of C=C stretching vibration at 1637  $\text{cm}^{-1}$ . Compared with the spectrum of AM, the spectra of Tyr/Trp-MIPs both before and after extraction showed a single absorption peak at 3446  $\text{cm}^{-1}$ , suggesting that the primary amide of AM was translated into the secondary amide after polymerization. The polymerization made the absorption intensity for C=C stretching vibration at 1635  $\text{cm}^{-1}$  weaker, which could be attributed to the transform from C=C in EDMA and AM to C–C in Tyr/Trp-MIPs. These results confirmed that Tyr/Trp-MIPs were successfully synthesized using AM as the functional monomer and EDMA as the cross-linker. However, from the FT-IR spectra, it was difficult to determine whether the templates were removed after extraction because of the indistinguishable characteristics of the carbonyl stretches corresponding to the templates and the bulk polymer.<sup>28</sup>

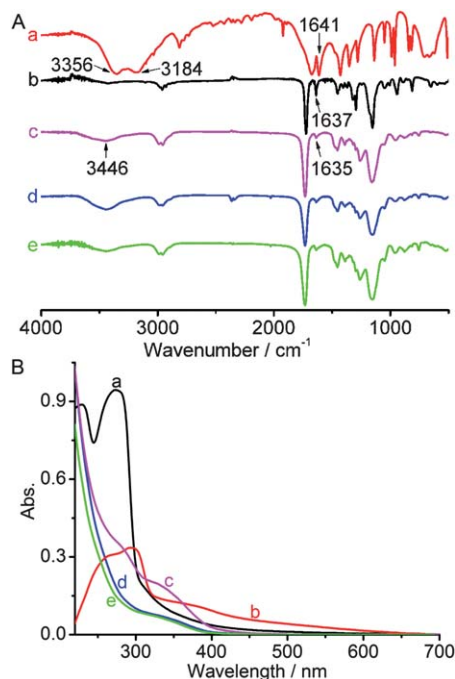


**Fig. 3** (A) FT-IR spectra of AM (a), EDMA (b), Tyr/Trp-MIP (c) before and (d) after extraction, and NIP (e). (B) Solid-state UV-vis absorption of L-Tyr (a), L-Trp (b), Tyr/Trp-MIP (c) before and (d) after extraction, and NIP (e).

To confirm the removal of the template after extraction, solid-state UV-vis spectra of L-Tyr, L-Trp, Tyr/Trp-MIPs before and after extraction, and NIP were compared (Fig. 3B). L-Tyr and L-Trp showed UV-vis absorption at 296 and 275 nm, respectively, while Tyr/Trp-MIP showed a wide absorption band in the range from 250 to 400 nm. The shift of the absorption peaks corresponding to L-Tyr and L-Trp indicated the interactions among the templates and the specific recognition sites of MIP. After extraction the Tyr/Trp-MIP showed lower UV-vis absorbance in the range from 250 to 400 nm than that before extraction, the absorption of Tyr and Trp nearly disappeared, and the UV-vis spectrum was similar to that of NIP, indicating the efficient removal of the templates upon extraction.

### Properties of microchip

The microchip could conveniently be constructed by fixing a multi-template imprinted capillary in a PDMS substrate. The preparation of imprinted capillary prior to microchip construction avoided the effect of heating process in the preparation of PDMS on the recognition ability of MIP. More importantly, the length and inner diameter of the separation channel could be conveniently regulated for obtaining the best separation performance, and the microchip was low-cost and disposable.

The MIPs were one-pot synthesized and directly attached on the capillary wall by covalent bonding of the polymer to silanol group. Thus the imprinting process avoided many problems occurred in conventional filling methods for preparation of molecularly imprinted separation column, *i.e.*, irregular MIP particle packing, frit making as well as bubble formation. Moreover, the MIP-coated microchannel was stable, and a single synthesis step could form a MIP with 2-fold predetermined selectivity for two couples of chosen analytes, which was advantageous to the miniaturization of separation system. With the MIP-based microchip, simultaneous multiple enantioseparation could be achieved in a short time.

### Detection potential

The electrochemical oxidation of Tyr and Trp enantiomers at a carbon fiber microdisk electrode produced detectable amperometric signal. When the applied potential was less than +0.6 V, no signal could be observed for Tyr and Trp enantiomers. With the increasing applied potential from +0.6 to +1.2 V the amperometric responses increased, and a quick increase occurred at potentials more positive than +1.0 V. When the applied potential was higher than +1.2 V the oxidation currents increased slowly and the baseline became noisy and unstable. Thus, +1.2 V was used as the optimum detection potential.

### Optimization of chiral separation conditions

The effects of ACN content, pH and concentration of acetate buffer on  $I_s$  of Tyr and Trp enantiomers are shown in Fig. 4. ACN is the most extensively used additive in mobile phase due to its low viscosity. The retention times of two couples of enantiomers reduced with increasing ACN content, which resulted from the increasing electroosmotic flow (EOF),<sup>42</sup> while high ACN level favours the imprinting effect.<sup>31,43</sup> Thus  $I_s$  increased with the ACN content changing from 80% to 95% (Fig. 4A). However, the short

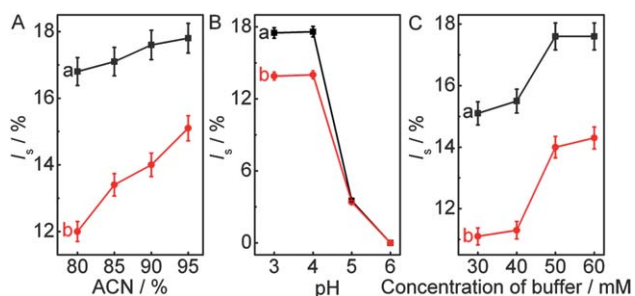


**Fig. 4** Effects of (A) ACN content, (B) pH and (C) concentration of acetate buffer on  $I_s$  for (a) racemic Tyr and (b) racemic Trp at a separation voltage of 1200 V.

retention times made the value of  $\Delta t_R$  smaller. Considering the retention times and  $I_s$ , an ACN content of 90% (v/v) in the mobile phase was chosen, at which effective enantiomer separation could be achieved.

The pH of mobile phase is an important issue since it alters both the charges of the analytes and the polymer, thus affecting the molecular recognition of the analytes, as well as the EOF.<sup>43</sup> With the increasing pH value from 3.0 to 6.0, both the retention times of two couples of enantiomers decreased due to the increasing EOF and weakening interaction between the enantiomers and functional groups on the surface of MIP. In addition, the  $I_s$  of these enantiomers showed the stable values in the pH range from 3.0 to 4.0 and then decreased (Fig. 4B). At the pH value of 4.0, both the retention times and the  $I_s$  were suitable, and  $\Delta t_R$  was large enough to separate the two couples of enantiomers, thus pH 4.0 was used for simultaneous multiple enantio-separation.

Fig. 4C shows the effect of concentration of acetate buffer on the selectivity of the MIP. With the increasing concentration, the retention times of two couples of enantiomers continuously increased due to the decreasing EOF and elution ability,<sup>42</sup> while the  $I_s$  increased and reached the platforms after 50 mM. Thus the concentration of 50 mM was selected as the optimal condition concerning both short retention times and large  $I_s$  values.

### Enantioseparation of racemic Tyr and Trp

The Tyr/Trp-imprinted microchip showed simultaneous baseline separation for both racemic Tyr and Trp within 120 s with  $R_s$  values of 1.02 and 1.00 for Tyr and Trp, respectively (electrochromatogram a, Fig. 5A). The two couples of dual peaks were attributed to the specific recognition of MIP toward L-Tyr and L-Trp. As a control, the electrochromatograms for enantio-separation of individual racemic Tyr and racemic Trp on the Tyr/Trp-imprinted microchip showed one pair of peaks for D-Tyr and L-Tyr, and D-Trp and L-Trp, respectively (electrochromatograms b and c, Fig. 5A). The separation efficiency changed with the different capillary-integrated microchips (Fig. 5B). On bare capillary-integrated and NIP-imprinted capillary-integrated microchips, the mixture of racemic Tyr and racemic Trp showed only two single peaks, thus they were impossible to be used for enantio-separation. The longer retention times on NIP-imprinted capillary-integrated microchip resulted from the unspecific interaction between the enantiomers and the MIP. In the

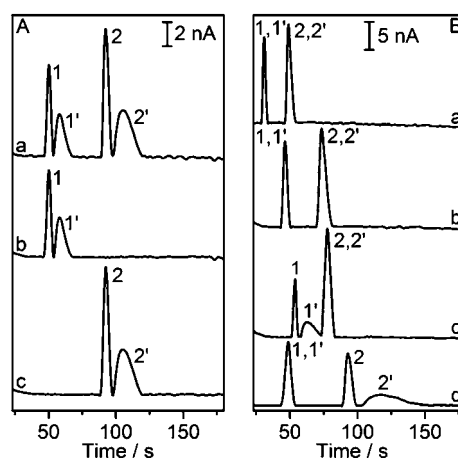


**Fig. 5** (A) Electrochromatograms for enantio-separation of (a) racemic Tyr and Trp, (b) racemic Tyr and (c) racemic Trp on Tyr/Trp-imprinted microchip, and (B) electrochromatograms for enantio-separation of racemic Tyr and Trp on microchips with (a) bare, (b) NIP-coated, (c) Tyr-imprinted and (d) Trp-imprinted microchannels. Peak identity: 1, D-Tyr; 1', L-Tyr; 2, D-Trp; 2', L-Trp.

presence of single-templated MIPs, both racemic Tyr and racemic Trp could not be baseline separated on Trp- and Tyr-imprinted microchips due to the absence of recognition sites complementary to L-Trp and L-Tyr, respectively. These results confirmed that only the Tyr/Trp-MIP coated microchannel could separate the enantiomers of Tyr and Trp in one single run.

### Quantitative detection and reproducibility

As discussed above, amperometry using carbon fiber microdisk electrode at +1.2 V (*vs.* Ag/AgCl) was selected for quantitative detection owing to the excellent electroactivity of these analytes and path length-independent and low-cost measurement, which showed two couples of dual peaks of these enantiomers. All

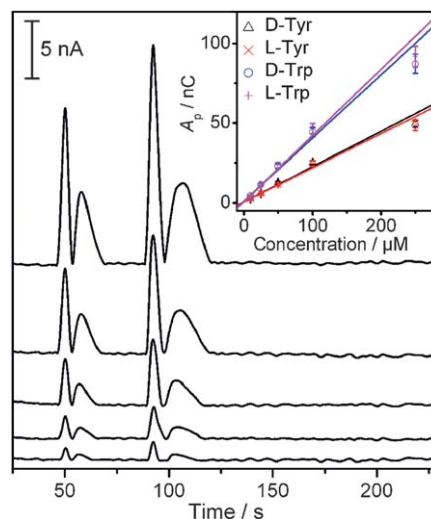


**Fig. 6** Electrochromatograms of racemic Trp and Tyr at the concentrations of 20, 50, 100, 200 and 500  $\mu\text{M}$  from bottom to top. Inset: calibration curves for D-Tyr, L-Tyr, D-Trp and L-Trp detection under optimal conditions.

**Table 2** Separation and detection reproducibility of the imprinted microchip for Tyr and Trp enantiomers under optimal conditions ( $n = 6$ )

Analytes	RSD (%) of $t_M$			RSD (%) of $A_p$		
	Run-to-run	Day-to-day	Chip-to-chip	Run-to-run	Day-to-day	Chip-to-chip
D-Tyr	1.2	2.7	3.8	2.6	4.3	5.9
L-Tyr	1.5	2.4	3.9	3.9	6.7	8.6
D-Trp	1.5	2.7	5.0	3.8	6.9	8.5
L-Trp	1.8	2.7	5.2	3.9	7.1	8.8

amperometric responses increased with increasing concentration of racemic Tyr and Trp (Fig. 6). The linear ranges for D-Tyr, L-Tyr, D-Trp and L-Trp were from 10 to 250  $\mu\text{M}$  with relative coefficients of 0.993, 0.994, 0.991 and 0.992, respectively (inset in Fig. 6). The detection limits at the S/N ratio of 3 were 2.0, 4.0, 1.5 and 4.0  $\mu\text{M}$  for D-Tyr, L-Tyr, D-Trp and L-Trp, respectively. Considering the sampling volume less than 0.39 nL,<sup>37</sup> the designed method could detect the enantiomers down to 0.58 fmol.

The relative standard deviations (RSD) ( $n = 6$ ) of  $t_R$  of D-Tyr, L-Tyr, D-Trp and L-Trp were from 1.2% to 1.8% for run-to-run, 2.4% to 2.7% for day-to-day, and 3.8% to 5.2% for chip-to-chip, respectively (Table 2). The RSD ( $n = 6$ ) of peak areas measured at 200  $\mu\text{M}$  racemic Tyr and 200  $\mu\text{M}$  racemic Trp were from 2.6% to 3.9% for run-to-run, 4.3% to 7.1% for day-to-day, and 5.9% to 8.8% for chip-to-chip (Table 2). These results suggested that the proposed method had good stability and precision, and the imprinted microchips had good fabrication reproducibility.

## Conclusions

A chip-based simultaneous multiple enantioseparation method was designed with a multi-template imprinted microchannel. The imprinted microchannel was formed by one-pot synthesis of multi-template MIP on silanized capillary wall, which led to chemical attachment of the MIP and could avoid many problems in conventional methods for construction of imprinted separation channel. The imprinted capillary as the separation microchannel was open-tubular and could be conveniently regenerated by efficient removal of the templates with an extraction step. Furthermore, its length and inner diameter could be conveniently regulated for obtaining the best separation performance. The imprinted microchip was low-cost and disposable, and showed excellent separation efficiency for achieving simultaneous enantioseparation of two couples of enantiomers, racemic Tyr and racemic Trp, in a short time. By applying a potential of +1.2 V (*vs* Ag/AgCl), the separated enantiomers could directly be quantitatively detected with good sensitivity, which avoided the problems occurred in other indirect methods. The designed method could be extended for simultaneous separation of more pairs of enantiomers, thus opened a promising avenue for high-throughput screening of chiral compounds.

## Acknowledgements

We gratefully acknowledge the financial support of the National Basic Research Program of China (2010CB732400) from the

Ministry of S&T and the National Natural Science Foundation of China (20821063, 20835006, 90713015, 20875044).

## References

- 1 K. Hamase, A. Morikawa and K. Zaitzu, *J. Chromatogr., B*, 2002, **781**, 73–91.
- 2 V. Guillén-Casla, M. E. León-González, L. V. Pérez-Arribas and L. M. Polo-Díez, *Anal. Bioanal. Chem.*, 2010, **397**, 63–75.
- 3 H. Wolosker, S. Blackshaw and S. H. Snyder, *Proc. Natl. Acad. Sci. USA*, 1999, **96**, 13409–13414.
- 4 T. Nishikawa, *Biol. Pharm. Bull.*, 2005, **28**, 1561–1565.
- 5 T. Furuchi and H. Homma, *Biol. Pharm. Bull.*, 2005, **28**, 1566–1570.
- 6 A. D'Aniello, *Brain Res. Rev.*, 2007, **53**, 215–234.
- 7 K. Hamase, A. Morikawa, S. Etoh, Y. Tojo, Y. Miyoshi and K. Zaitzu, *Anal. Sci.*, 2009, **25**, 961–968.
- 8 H. Brückner and A. Schieber, *Biomed. Chromatogr.*, 2001, **15**, 166–172.
- 9 B. V. Wickern, B. Müller, T. Simat and H. Steinhart, *J. Chromatogr., A*, 1997, **786**, 57–65.
- 10 L. Qi, Y. L. Han, M. Zuo and Y. Chen, *Electrophoresis*, 2007, **28**, 2629–2634.
- 11 L. Qi, M. R. Liu, Z. P. Guo, M. Y. Xie, C. G. Qiu and Y. Chen, *Electrophoresis*, 2007, **28**, 4150–4155.
- 12 K. Hamase, Y. Miyoshi, K. Ueno, H. Han, J. Hirano, A. Morikawa, M. Mita, T. Kaneko, W. Lindner and K. Zaitzu, *J. Chromatogr., A*, 2010, **1217**, 1056–1062.
- 13 A. A. Adoubel, C. J. Morin, N. Mofaddel, G. Dupas and P. L. Desbène, *Anal. Bioanal. Chem.*, 2009, **394**, 597–608.
- 14 S. Anouti, O. Vandenabeele-Trambouze, D. Koval and H. Cottet, *Electrophoresis*, 2009, **30**, 2–10.
- 15 X. Z. Wang, X. F. Yin, H. Y. Cheng and H. Shen, *Analyst*, 2010, **135**, 1663–1671.
- 16 M. Vázquez, C. Frankenfeld, W. K. T. Coltro, E. Carrilho, D. Diamond and S. M. Lunte, *Analyst*, 2010, **135**, 96–103.
- 17 G. Fercher, A. Haller, W. Smetana and M. J. Vellekoop, *Analyst*, 2010, **135**, 965–970.
- 18 R. E. Holcom, J. R. Kraly and C. S. Henry, *Analyst*, 2009, **134**, 486–492.
- 19 C. Nilsson, S. Birnbaum and S. Nilsson, *J. Chromatogr., A*, 2007, **168**, 212–224.
- 20 A. B. Jemere, R. D. Oleschuk and D. J. Harrison, *Electrophoresis*, 2003, **24**, 3018–3025.
- 21 H. L. Zeng, H. F. Li and J. M. Lin, *Anal. Chim. Acta*, 2005, **551**, 1–8.
- 22 S. I. Cho, J. Shim, M. S. Kim, Y. K. Kim and D. S. Chung, *J. Chromatogr., A*, 2004, **1055**, 241–245.
- 23 S. Nagl, P. Schulze, M. Ludwig and D. Belder, *Electrophoresis*, 2009, **30**, 2765–2772.
- 24 N. Piehl, M. Ludwig and D. Belder, *Electrophoresis*, 2004, **25**, 3848–3852.
- 25 P. Qu, J. P. Lei, R. Z. Ouyang and H. X. Ju, *Anal. Chem.*, 2009, **81**, 9651–9656.
- 26 S. A. Zaidi, K. M. Han, D. G. Hwang and W. J. Cheong, *Electrophoresis*, 2010, **31**, 1019–1028.
- 27 J. J. Ou, X. Li, S. Feng, J. Dong, X. L. Dong, L. Kong, M. L. Ye and H. F. Zou, *Anal. Chem.*, 2007, **79**, 639–646.
- 28 H. F. Wang, Y. Z. Zhu, X. P. Yan, R. Y. Gao and J. Y. Zheng, *Adv. Mater.*, 2006, **18**, 3266–3270.
- 29 S. A. Zaidi and W. J. Cheong, *J. Chromatogr., A*, 2009, **1216**, 2947–2952.
- 30 S. A. Zaidi and W. J. Cheong, *Electrophoresis*, 2009, **30**, 1603–1607.
- 31 L. Schweitz, L. I. Andersson and S. Nilsson, *J. Chromatogr., A*, 1997, **792**, 401–409.
- 32 L. Schweitz, *Anal. Chem.*, 2002, **74**, 1192–1196.
- 33 P. Spégl, L. Schweitz and S. Nilsson, *Anal. Chem.*, 2003, **75**, 6608–6613.
- 34 A. C. Meng, J. LeJeune and D. A. Spivak, *J. Mol. Recognit.*, 2009, **22**, 121–128.
- 35 L. Sabourin, R. J. Ansell, K. Mosbach and I. A. Nicholls, *Anal. Commun.*, 1998, **35**, 285–287.
- 36 M. Pumera, *Electrophoresis*, 2007, **28**, 2113–2124.
- 37 C. Zhai, C. Li, W. Qiang, J. P. Lei, X. D. Yu and H. X. Ju, *Anal. Chem.*, 2007, **79**, 9427–9432.

- 
- 38 H. S. Andersson, J. G. Karlsson, S. A. Piletsky, A. C. Koch-Schmidt, K. Mosbach and I. A. Nicholls, *J. Chromatogr., A*, 1999, **848**, 39–49.
- 39 C. Zhai, W. Qiang, J. P. Lei and H. X. Ju, *Electrophoresis*, 2009, **30**, 1490–1496.
- 40 C. Yu and K. Mosbach, *J. Mol. Recognit.*, 1998, **11**, 69–74.
- 41 O. Brüggemann, R. Freitag, M. J. Whitcombe and E. N. Vulfson, *J. Chromatogr., A*, 1997, **781**, 43–53.
- 42 J. J. Ou, J. Dong, T. J. Tian, J. W. Hu, M. L. Ye and H. F. Zou, *J. Biochem. Biophys. Methods*, 2007, **70**, 71–76.
- 43 Z. S. Liu, C. Zheng, C. Yan and R. Y. Gao, *Electrophoresis*, 2007, **28**, 127–136.